Fluidized bed with sensors for eco-friendly plasma disinfection of seeds

Subgroup thesis report Bachelor Graduation Project

July 20, 2024

Delft University of Technology

Student Name	Student Number
Paul F. Lee	5529352
Thomas Ritmeester	5601371

Instructors:	dr.ing. H.W. van Zeijl, Prof.dr.ir. J. van Turnhout and dr. L. Wymenga
Project Duration:	April, 2024 - July, 2024
Faculty:	Faculty of Electrical Engineering, Mathematics, and Computer Science, TU Delft
Project partner:	Bejo Zaden b.v.

Abstract

Disinfection of seeds is a method used by the seed industry to remove pathogens. However, conventional methods have their shortcomings in terms of energy efficiency and yield. This thesis focuses on the design of a fluidized bed setup with sensors for the purpose of DBD plasma disinfection. Two configurations were investigated, namely a spouted bed and a bubbling fluidized bed, where the bubbling fluidized bed produced the best results. Additionally, the fluidized bed was equipped with motor speed control, and with sensors for the measurement of ozone concentration, temperature, humidity, air speed, and ion density. These sensors were integrated in an easy readout system using displays, making the system ready for testing of disinfection performance.

Acknowledgements

The authors wish to heartily thank our supervisors dr.ing. H. van Zeijl, Prof. dr. ir. J. van Turnhout, and Drs. L. Wymenga for their support, guidance, and feedback during the project. Thank you H. van Zeijl for arranging juries for our greenlight presentation. Thank you J. van Turnhout for arranging the trip to the Faculty Applied Sciences, which was key to our understanding of the principles of fluidization. Thank you L. Wymenga for your guidance in our lab experiments, and for kindly lending us your equipment.

A big thank you also goes out to Bejo Zaden B.V., for partnering in this project. Thank you B. Compaan and Y. Bakker for the warm welcome at the company, and thank you for attending meetings and presentations along the way.

Further thanks are owed to Dr. C. Viellard-Boutry for attending our greenlight presentation, to M. Schumacher and T. Slats for their lab support, to D. Bosma for guiding us in the lab facilities at the Faculty of Applied Sciences, and to our families for their support.

Contents

1 Introduction

1.1 Project objective

The agriculture industry has become more advanced over the years. From mechanized agriculture speeding up processes by orders of magnitude, to selectively breeding crops to be more resilient and plentiful. The advances in agriculture have been crucial in sustaining the growing world population. With food demands expected to rise even more over the next decades, new methods are sought to further increase crop yields.

The base of crop growth is the humble seed. Around this humble seed, a large industry has grown, specialized in breeding crops to enhance their properties, but also in treating the seeds themselves. For instance, seeds are treated with either a protective or non-protective layer, for improving ease of handling by machines, or containing pesticides, fertilizers, or microbes [1].

Quite another way of treating seeds is by disinfection. Disinfection is a necessary practice, since the warm and humid conditions needed for plant growth are also the ideal habitat for bacteria and fungi to flourish. However, the currently popular methods of disinfecting seeds are far from perfect. Hot water or chemical treatments are energy inefficient and wasteful processes, that may have negative effects on seed germination [2]. Therefore, science has been looking for more eco-friendly ways to disinfect seeds.

A promising new technology is plasma disinfection using cold plasma. Plasma disinfection is an effective way of disinfecting due to the reactive species the plasma creates. It has proven to be an effective disinfection method [3, 4]. Therefore, this thesis focuses on investigating a novel way to implement plasma disinfection unit using fluidized bed technology.

This thesis describes the design, implementation, and testing of a fluidized bed with sensors for the purpose of plasma disinfection of seeds. The fluidized bed provides a little explored way of disinfecting seeds using cold plasma. The project is specifically interested in the disinfection of cabbage seeds and disinfection of *Xanthomonas* bacteria and *Alternaria* spores. The project was done with two other project groups: one focusing on the creation of a high voltage power supply for plasma generation [5], and the other working on a novel design of plasma electrode for creating DBD plasma [6].

This project was done with support from our sponsor: Bejo Zaden B.V., an industry leader in collection, disinfection, and distribution of seeds.

1.2 State of the art analysis

Seed disinfection is currently performed using several different methods. One conventional method is using hot water bath treatment. This methods uses 50-60°C water baths for a duration of 10-30 minutes [7]. The hot water is highly effective against typically hard to eliminate pathogens, and for this reason the technique is used across the industry. Although this method is effective in disinfecting seeds, it is not that energy efficient. Therefore, other alternatives are being developed, such as plasma disinfection.

Plasma is in essence ionized gas. There are two main categories: thermal plasma, and non-thermal plasma, also known as cold plasma. For seed treatment, cold plasma is the most applicable option, since high temperatures have a negative effect on seeds. Several other benefits make cold plasma stand out: the treatment is possible at atmospheric pressure, it has lower energy consumption than thermal plasma, effective surface disinfection, and improved germination rates [8]. Plasma is a good disinfection agent, primarily because it produces ozone and the hydroxyl radical, which are strong oxidants [9]. As

oxidants, they deteriorate the cell membrane of (unwanted) organisms, effectively killing them [9, 10]. This results in disinfected surfaces.

Within plasma disinfection, there are also several ways in which the disinfection is applied. In [11], seeds were placed underwater and subjected to a DC arc discharge. Also in [11], seeds were placed in between two electrodes and subjected to DBD discharge from AC. In [12], seeds were placed on top of a co-planar DBD in an orbital shaker, with astounding disinfection efficiencies of 90% at 400W for 1 second, and 100% at 400W for 20 seconds. This high success rate makes plasma disinfection an attractive option.

A final method of implementing plasma disinfection, namely the method this thesis focuses on, is plasma disinfection using a fluidized bed. This was implemented by Dasan [13] using a spouted bed using hazelnuts. In his setup, a plasma jet was injected in a cylindrical reactor. Another fluidized bed setup was created by Măgureanu [14], where a volume dielectric barrier discharge was realized by a high voltage electric field across the cylindrical chamber in which fluidization of seeds took place.

It is important to mention that the combination of plasma with the fluidized bed is subject to many different applications besides disinfection, ranging from metallurgy, gasification of fuels, sterilization of food, and applying chemical coatings to particles [15]. The application of pulsed dielectric barrier discharge (DBD) for coating seeds with SiO_2 was already seen in 2006, though at small scale [16].

1.3 Thesis outline

This thesis is structured as follows. First, a general theoretical overview is given about plasma disinfection and fluidization theory. Next, the construction and design of the fluidized bed itself is discussed, after which the use and implementation of sensors is dealt with and the setup is tested with seeds. Finally, the discussion, conclusions, and recommendations are given.

2 Fluidization theory

Fluidization is the process of injecting a fluid (usually a gas) into a bed of particles, which makes the particulate substance behave like a fluid. Such a system is called a fluidized bed. Due to the high level of contact between the gas and solid, fluidized beds have applications in reactors and drying applications. For instance, fluidized beds are used for the production of chemicals, coating of particles, or used for drying seeds. Due to the perfect mixing of particles, fluidized beds have also successfully been used for seed disinfection purposes using steam [17] and plasma [13].

Fluidization behavior of particles changes depending on the size of the solid and its density. Geldart described four different fluidization classes of particles in [18], each having different properties. These classes can be seen in Figure 1. Looking at the figure and comparing the density of seeds around

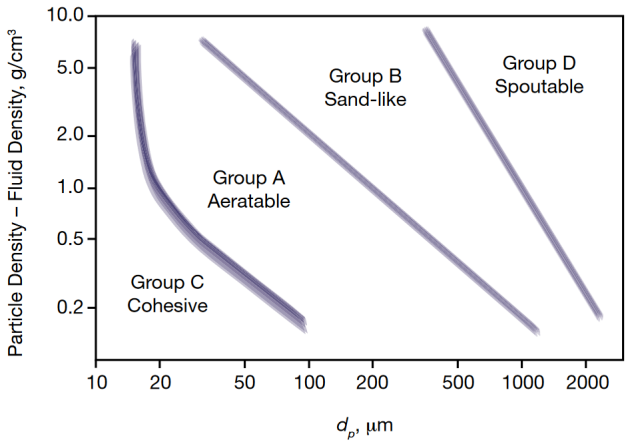

Figure 1: The four fluidization regions as described by Geldart [18]. Image sourced from [19].

$1g/cm^3$, and a particle size above 1000 micron to the graph, we find that the regions of interest for fluidization of seeds are group D: spoutable solids (and possibly group B: sand-like particles for smaller seeds, but this research document will focus on class D solids). Fluidization of these solids can be implemented using different methods, but we will further focus on two configurations: spouting and bubbling fluidized beds.

Bubbling fluidized beds are a popular method of implementing fluidized beds, realized by creating an uniform airflow through the entire surface of particles. This is usually done by laying a bed of particles on a perforated or porous plate, and pumping gas through it at a constant rate. An advantage of this topology is that the intense movement of particles provides good mixing [20]. Additionally, the system is easily scalable.

The second topology considered in this document is the spouting topology. This configuration is often used for class D "spoutable" particles, since larger particles are more difficult to fluidize due to a higher required fluidization velocity of the gas. The advantage of this technology is that larger particles can easily be fluidized, even on larger scale, but may have worse mixing performance than other types of fluidized beds due to the creation of dead zones with non-recirculating seeds [21].

3 Requirements

For the construction of the fluidized bed prototype, a set of requirements was created. This was done to define the scope of the build, as well as to ensure integration with the other components of the system, namely the developed plasma electrodes and high voltage power supply. The requirements were split up into two categories: those for the fluidized bed, and those for the sensor system. Additionally, the requirements are classified as either mandatory (*MR*) and trade-off (*ToR*) requirements.

Fluidized bed

1. The fluidized bed must provide either bubbling or spouting behaviour. (MR)
2. The fluidized bed must have the ability to fluidize cabbage (*Brassica*) seeds sized 1.75-2mm. (MR)
3. The fluidized bed must realize an air speed of a minimum of 0.5m/s inside the seed fluidization space. (MR)
4. The seed chamber must have a volume of 20x10x20cm (lxwxh). (MR)
5. The air used for fluidization should have the option to recirculate air. (ToR)
6. The fluidized bed must include a method of mounting a maximum of five electrodes of 10x10cm inside the seed chamber. (MR)
7. The fluidized bed setup must include a mounting solution for sensors that prevents interference with electrodes. (MR)
8. The fluidized bed must be constructed using materials that are resistant to the reactive molecules and ions created by DBD plasma. (ToR)

Sensors

9. The system must have sensors with which to measure the environmental conditions inside the setup. In order of descending priority, these include:
    - 9.1. Ozone concentrations of 0-100ppm (MR)
    - 9.2. Relative humidity of 0-90% (ToR)
    - 9.3. Temperature from 0-100°C (ToR)
    - 9.4. Air flow rate of 0-15m/s (ToR)
    - 9.5. Ion concentration up to $5 \cdot 10^6$ ions/cm^3 (ToR)
10. The system must implement a readout method for reading the sensor values, directly and/or using an external computer. (MR)

4 Fluidized bed

4.1 Introduction

For the disinfection of seeds, it is important that all seeds are treated evenly on all sides. For this reason, a fluidized bed was created. A fluidized bed is a system in where teh right conditions are created in order for granular materials to behave as a fluid. Typically, fluidization is realized by pumping pressurized gas through the particles. Fluidization is an excellent way of implementing plasma treatment of seeds, since the gases and reactive species created by a plasma can evenly treat a large number of seeds. In this section, the design, construction, and the choices made in doing so will be discussed. First, a series of calculations and experiments were done to inspect the fluidization behaviour of the seeds. Using this knowledge, the right components were chosen and both a bubbling and spouted fluidized bed were designed in CAD, and constructed accordingly.

4.2 Theory and experiments

In order to construct a fluidized bed, the fluidization behaviour of seeds needed to be known. To do this, there are several experimentally obtained equations from which the required fluidization velocity of the seeds can be derived. One popular equation is based on the work of Wen and Yu [22] (Equation 1). Using the properties of the seeds for which the fluidized bed was constructed, namely 1.75-2.00mm cabbage *Brassica* seeds, the derived minimum fluidization velocity can be found using this equation:

$$U_{mf} = \frac{\mu_g}{\rho_g d_p}(\sqrt{33.7^2 + 0.0408Ar} - 33.7) \tag{1}$$

Where μ_g is the viscosity of air, ρ_g the density of air, d_p the diameter of the particles to fluidize and Ar the Archimedes number, as found as in Equation 2. All relevant values can be found in Table 1.

$$Ar = \frac{\rho_g d_p^3 g(\rho_s - \rho_g)}{\mu_g^2} \tag{2}$$

Combining these two equations and filling in the values as given in Table 1 yields:

$$U_{mf} = \frac{1.81 \cdot 10^{-5}}{1.29 \cdot 0.0020}(\sqrt{33.7^2 + 0.0408 \cdot 2.46 \cdot 10^5} - 33.7) = 0.505 m/s \tag{3}$$

Symbol	Variable name	Used value
μ_g	Viscosity of fluid (air)	$1.81 \cdot 10^{-5} Pa \cdot s$
ρ_g	Density of fluid (air)	$1.29 kg/m^3$
ρ_s	Density of solid (seeds)	$795 kg/m^3$
d_p	Particle diameter	$2.0 mm$
g	Gravitational acceleration	$9.81 m/s^2$
Ar	Archimedes number (seeds in air)	$2.46 \cdot 10^5$

Table 1: Parameters used in calculating the minimum fluidization velocity of *Brassica* seeds in air.

Other empirical equations for the minimum fluidization velocity, like those by Richardson *et al* [23], yield similar vales for minimum fluidization velocity.

Besides theoretically determining the required values for the design of the fluidized bed, the values were also determined experimentally at the TU Delft Faculty of Applied Sciences. This was done using a general fluidization setup, consisting of a glass column with a porous plate at the bottom (see Table 2 for the setup parameters). At the bottom, an air inlet was connected, through which the flow

(a) The experimental setup used to determine the fluidization parameters of the seeds.

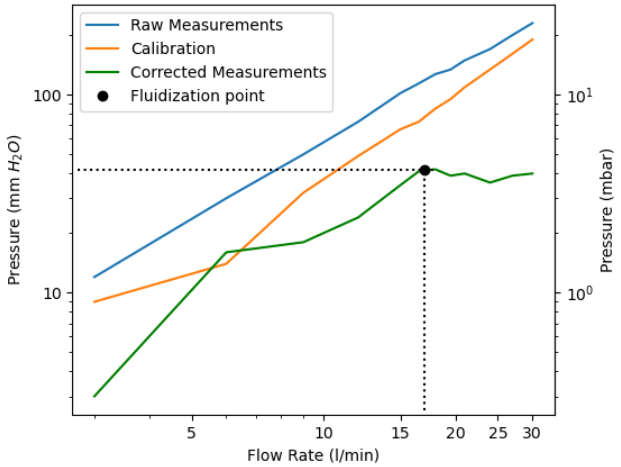

(b) The plotted measurements from the fluidization experiment.

Figure 2: The fluidization experimental setup and results.

of air can be precisely regulated using a mass flow controller. The experiment itself was performed by filling the column with seeds, and reading out the pressure using a water column manometer at different flow rates. The measurement results of experiment are found in Figure 2b. In the figure, the raw measurements are plotted where both the seeds and perforated plate were present. In orange, the calibration measurements with the perforated plate, and in green the final corrected measurements can be seen. From the experiment, a minimum fluidization velocity was found as the inflection point from where constant pressure occurs. From the corrected measurements, the constant pressure level occurred at flow rates above 17l/min, which corresponds to an air velocity of 0.57m/s. This value was close the theoretically determined value. Additionally, the constant pressure at fluidization was found to be around 40mm H_2O. Using these parameters, a suitable blower could be chosen for realizing fluidization.

Parameter	Value
Column diameter	$25.2mm$
Air flow rate range	$0 - 30l/s$
Bed height (rest)	$55mm$
Used seed volume	$30ml$
Seed bulk density	$710kg/m^3$
Seed diameter	$1.75 - 2.00mm$

Table 2: The parameters of the fluidized cabbage seeds and the fluidization setup.

4.3 Design of fluidized bed

4.3.1 Air flow control

For realizing a bubbling or spouted bed, a constant air flow needs to be realized. To do this, there are two main options: using a compressor with a mass flow controller, and using electric fans. Electric fans were chosen for the high air flow they provide, their cost-effectiveness, ease of use, and ease of implementing recirculation of air.

Within the fan classes, the choice for radial fans was made due to the high pressure air output they provide. This is in contrast to the classic axial fans that provide high airflow, but at lower pressures. The experiments from subsection 4.2 showed that the system needed an air pressure of 40mm H_2O and an air speed of 0.57m/s. For the setup with an area of 20x10cm, the required air flow rate would be $0.57m/s \cdot 0.2m \cdot 0.1m = 0.0114m^3/s = 0.684m^3/min$. To achieve this, the BFB1012VH-A radial fan [24] from Delta Electronics was chosen, since this fan is capable of delivering a substantial amount air flow of $0.30m^3/min$ at the desired static pressure. In the end, four of these fans were used in parallel to realize a bubbling fluidized bed. Although three fans would have provided enough airflow in theory, the addition of a perforated plate as a diffuser was expected to cause a pressure drop too, so an additional fan was used to compensate for this.

The speed of the fan could be regulated using a microcontroller. This feature was mainly implemented to have control over the power at which seeds are propelled during the spouting operation of the system. The fan speed was controlled using a PWM signal switching a logic level MOSFET at a frequency of 50kHz, with a duty cycle varying between 0 and 100%. This will be elaborated on further in section 6.

4.3.2 CAD design

The construction of the fluidized bed was done in CAD software SolidWorks, after which the design was fabricated using 3D printing and laser cutting. In the design of the fluidized bed, two fluidization configurations were considered, namely a bubbling and a spouting configuration. While there are alternatives, like a circulating and vibratory fluidized bed, these topologies were chosen since they have a precedent in seed treatment [13, 25] and were easy to implement.

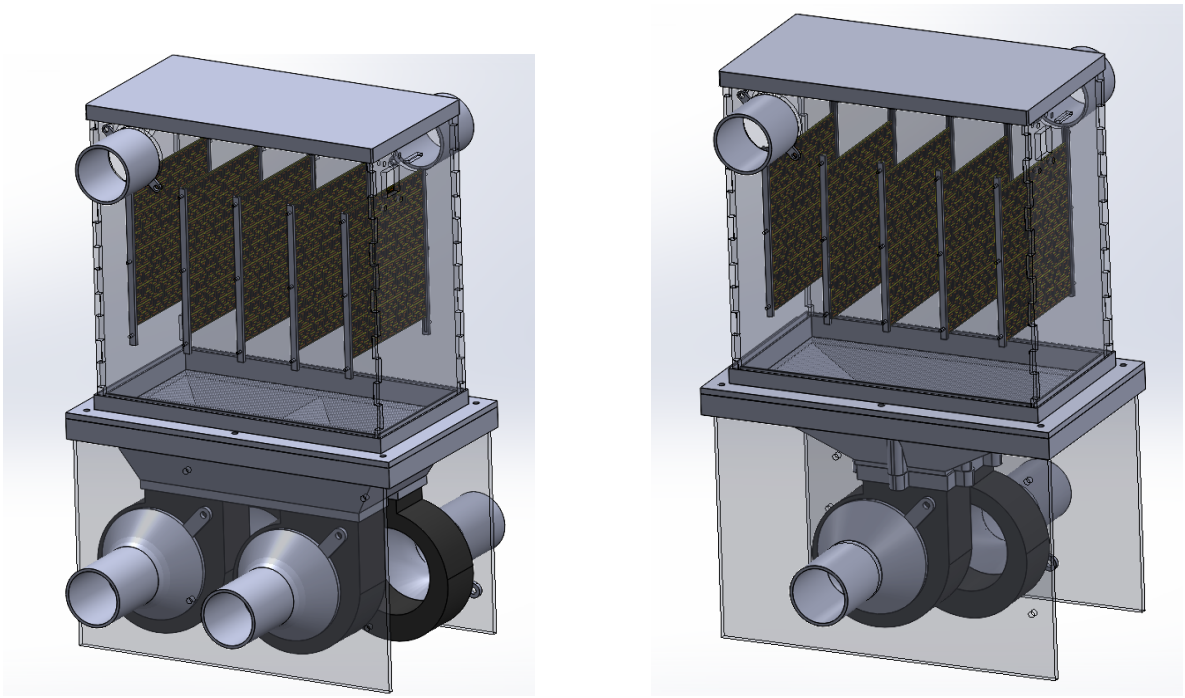

(a) CAD design of the fluidized bed in bubbling configuration (without optional recirculation pipes attached).

(b) CAD design of the fluidized bed in spouting configuration (without optional recirculation pipes attached).

Figure 3: CAD models of both fluidized bed configurations.

The bubbling configuration was realized by creating a 20x10x20cm transparent PMMA chamber in which the seeds are located. This material was chosen in particular due to high resistance to ozone. The seed chamber contains the mounting mechanism of the electrodes responsible for plasma disinfection. The seeds lay on top of a perforated plate with 1mm holes spaced at 2.54mm. Underneath this plate, the four radial fans are located, which blow air through the seeds. This design and constructed system can be seen in Figure 3a and Figure 4a, respectively.
The spouting configuration was realized in the same setup, but by creating a modified mounting mechanism for the fans. This time, only two fans were mounted side to side in a funnel shape, creating an approximately square region of air flow in the center. Note that for this configuration, no perforated plate was used, but rather a thin fiberglass mesh (0.2mm wire, 1.2mm spacing) that prevents seeds from entering the fans. The design and constructed system can be seen in Figure 3b and Figure 4b, respectively.

(a) Bubbling bed configuration with recirculation pipes attached.

(b) Spouted bed configuration with recirculation pipes attached.

Figure 4: The realized models of both fluidized bed configurations.

4.4 Results

Both configurations were tested using 1.75-2mm *Brassica* seeds at different fan power levels. Additionally, to find out to what extent the seeds mix, some colored seeds were put in the system to visualize the flow of seeds.

The bubbling bed showed promising results for mixing. A test was done with a layer of 25mm untreated seeds, and a 2mm layer of colored seeds. Although adequate mixing occurred within seconds, the setup was run for 45 seconds in total. The results can be found in Figure 5. As seen in the figure, the mixing performance was excellent overall, with some small deadzones were observed around the edges and corners. Seed movement was drastically reduced in these spots. This was most likely

occurring at the spots near the center of the radial fan, where less air is blown due to the centrifugal nature of the radial fans.

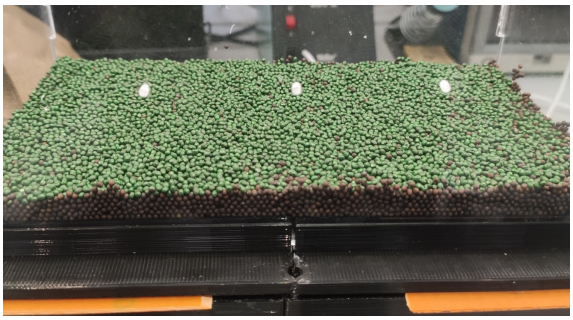

(a) Front view of the seeds before fluidization.

(b) Top view of the seeds before fluidization.

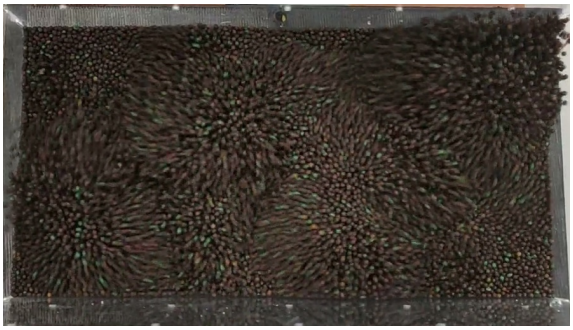

(c) Top view of seeds during fluidization.

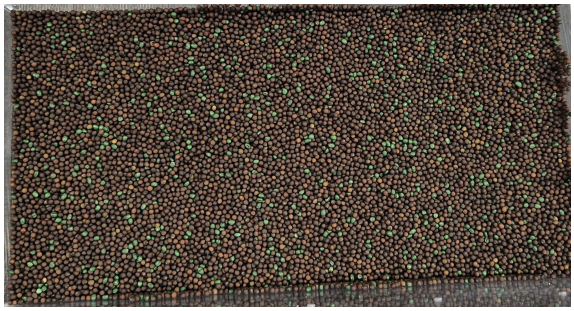

(d) Top view of the seeds after 45 seconds of fluidization.

Figure 5: Results of fluidization mixing test using the bubbling bed.

Additionally, some tests were performed to investigate the bubbling behaviour with different quantities of seeds. The tests were done with increments of 100ml seeds, up to 700ml. Each increment contributed approximately 5mm to the bed height. The different amounts of seeds changed the fluidization behaviour marginally, with low pressure spots becoming more visible by the lack of agitation of the seeds as more seeds were added. This resulted in slightly slower mixing at larger capacities. An empirical judgement is that, for our current setup, the optimum balance between treatment time and volume is achieved at roughly 500ml of seeds with the bubbling configuration.

The spouted bed showed decent results too. Seeds filled the volume well, but it was observed that there appeared deadzones when using larger amounts seeds. Since the seeds were propelled vertically, there was not much horizontal movement, resulting in some seeds being recirculated less than others, and a slower recirculation in general. The problems could be mitigated by using a lower quantity of seeds in the reactor, or letting the system run for longer, but this would reduce time efficiency and capacity of the system. However, the system performed well overall, providing decent mixing as evident in Figure 6.

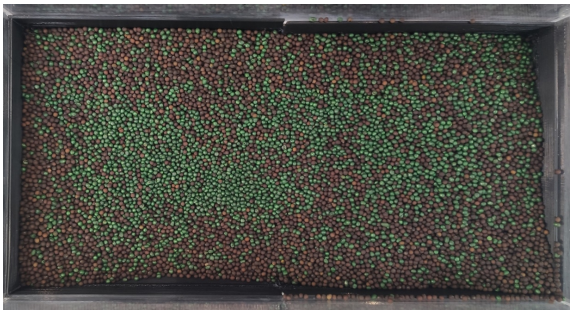

(a) Top view of the seeds before fluidization.

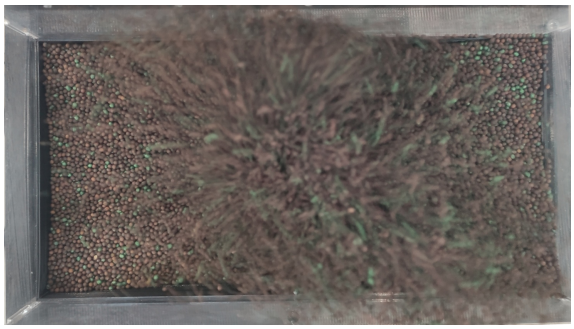

(b) Top view of the seeds during fluidization.

(c) Top view of the seeds after 45 seconds of fluidization.

Figure 6: Results of fluidization mixing test using the spouted bed.

The same tests with increasing quantities of seeds were performed with a spouted bed, starting with a 100ml of seeds, and increasing in increments of 100ml until 700ml was used. The spouting was initiated and sustained at a lower power as compared to bubbling bed at all seed quantities. Significant dead zones at the edges resulted in much slower mixing than in the bubbling configuration. An empirical judgement is that, in our current setup, the optimum balance between treatment time and volume is approximately 300ml for the spouting configuration.

4.5 Conclusions

For the main reactor of plasma disinfection, a bubbling fluidized bed was constructed. Using theoretical and experimental methods, the fluidization behaviour of the system was determined. Using the findings of these methods, a fluidized and spouted bed were constructed and tested. Both solutions, but especially the bubbling bed topology, proved to provide excellent mixing of seeds.

5 Sensors

5.1 Introduction

During operation of the plasma fluidized bed, there are several variables that require measuring. These include ozone concentration, air speed, relative humidity, and ion concentration. To answer to this and the requirements in section 3, the following sensors are implemented:

- Two ozone sensors, one low range (0-10ppm), and one high range (10-1000ppm)
- A mass flow sensor to measure air speed
- A temperature and humidity sensor
- An ion density meter

The justification behind choosing these sensors will be explained in their corresponding sections. Additionally, the fluidized bed is equipped with a microcontroller and a set of displays for easy readout of the data, as elaborated upon in section 6.

5.2 Mass flow sensor

The gas flow rate is an intrinsic property of a fluidized bed, as it is related to degree of fluidization as described earlier in subsection 4.2. As described in [15], flow rate also influences mixing of the seeds, the creation of so called 'dead zones' with little flow, and of thermal 'hot spots'. Additionally, if the airflow were to be blocked due to dust or debris, the flow sensor would be able to detect this before the machine is damaged. It is therefore instrumental to control the flow speed, which in turn requires a flow meter. As calculated in subsection 4.2, the desired flow velocity in the main chamber is an average of 0.5 meters per second in the main chamber. Since the seeds are expected to affect local flow velocity, the choice was made to place the flow sensor in the recirculation pipes, where approximately laminar flow is assumed. Additionally, the flow velocity would be higher inside the narrow recirculation pipes, giving a wider range speeds to measure. The desired sensitivity range of the flow sensor is then approximated with Equation 4, under the assumption that volume flow rate remains constant.

$$A_1 \cdot v_1 \ = \ A_2 \cdot v_2 <=> v_2 = \frac{A_1}{A_2} v_1 \tag{4}$$

Define A_1 to be the area of the main chamber, which is $0.1m \cdot 0.2m = 0.02m^2$. Then $v_1 = 0.684m/s$ is the previously calculated air flow velocity inside the main chamber. There are two re-circulation pipes, which each have a $0.04m$ diameter. Their combined area is then $2 \cdot \pi(\frac{0.04}{2})^2 = 0.0025133m^2$. Solving for v_2, the flow velocity in the re-circulation pipe, using Equation 4, $v2$ is found as $v_2 = 5.44m/s$.

To measure the air flow in the system, the fs7.a.1l.195 [26] was chosen (also see Figure 7a). This sensor is a small form factor sensor capable of measuring fluid flow between 0m/s and 40 m/s, and claims the highest sensitivity at lower flow speeds [27]. This is also evident in its nonlinear behaviour.

The sensor works using a small heater and a Pt1200 temperature sensor. The rate of cooling is related to the air speed flowing across the device, which changes the resistance of the sensor, which in turn can be converted into an electronic signal. The application note [27] suggested a constant temperature anemometer circuit using an operational amplifier. This allowed the temperature of the heater to be constant across a wide range of air speeds. The circuit can be found in Figure 7b. The output voltage of the circuit is related to air speed according to the following equation:

$$U = U_0\sqrt{1 + kv^n} \tag{5}$$

(a) The fs7.a.1l.195 mass flow sensor (image from product datasheet [26]).

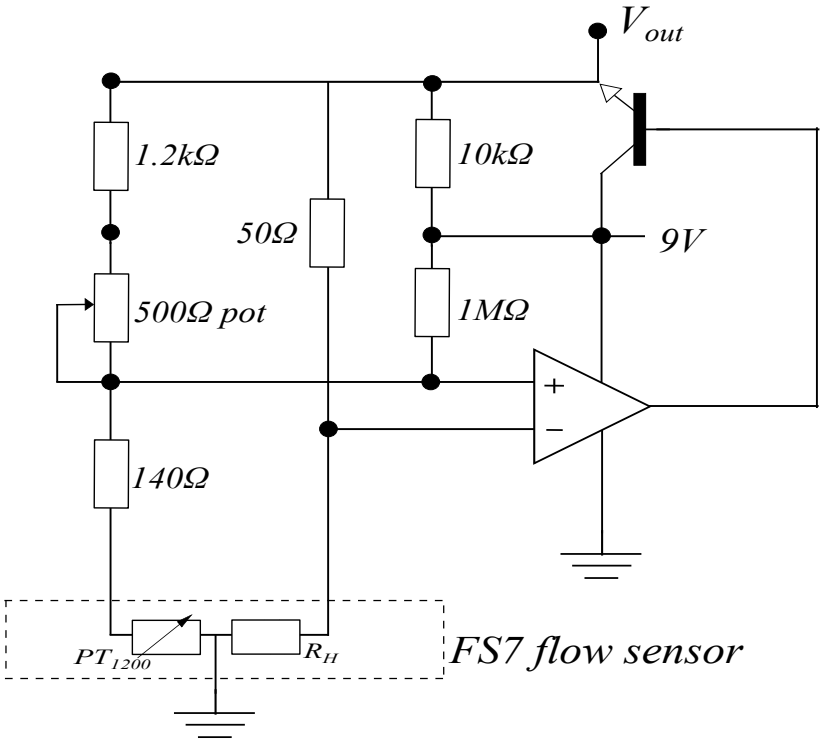

(b) Flow Sensor Readout Circuit, as found in the fs7.a.1l.195 [27] application note.

Where U is the output voltage, U_0 the output voltage at zero air speed, v air speed and k and n sensor and circuit constants found by calibration.

The circuit was calibrated according to the manufacturer's application note. This consisted of taking a three point calibration, to which a curve could be fit showing the relation between air speed and output voltage. The calibration was done by reading out the circuit's output voltage V_{out} at three points (minimum, maximum, and middle of air speed measurement range), and measuring the corresponding air speed using a commercial sensor. Using these values, the constants n and k were found, with which the calibration curve from Figure 8 was obtained. Additionally, a set of verification measurements were done, to check correct operation of the sensor.

5.3 Ion sensor

Plasma in essence is ionized gas [8]. Thus a logical method for quantifying plasma is by measuring the ion density of plasma activated air. To this end, an ion sensor was constructed. The amplifier design was modeled to that used in [28]. It consisted of a transimpedance amplifier followed by an inverting voltage amplifier. They put a voltage over both plates, treating it as a variable resistor whose resistance depends on the ion concentration of the air in between. This would result in a current feeding into the transimpedance amplifier, inducing a negative voltage at the output. Then they used the inverting voltage amplifier to invert back to a positive voltage for the analog to digital converter. The expectation was that our setup would yield similar results. However, a different kind of behaviour was observed.

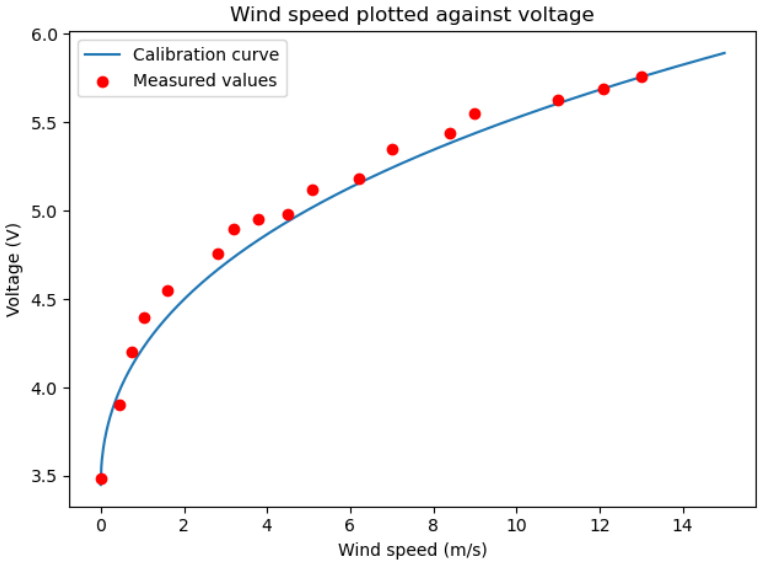

Figure 8: Flow Sensor calibration curve and test measurements.

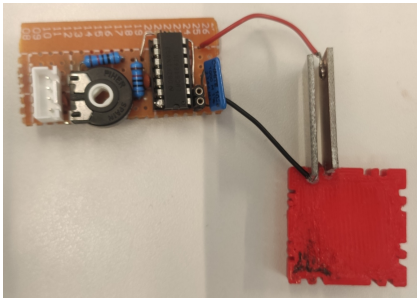

(a) The constructed ion sensor, with the amplifier circuit on the top-left, and the ion plates on the bottom-right.

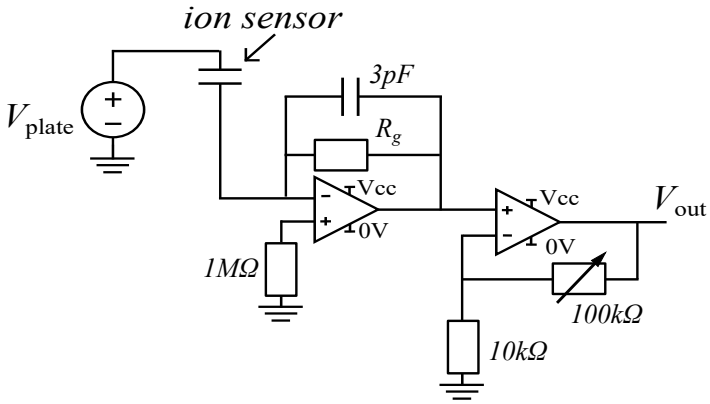

(b) Ion Sensor Circuit Diagram, modified from [28]

Figure 9: The construction of the ion sensor.

Without applying voltage across the plates, whilst aiming a commercial "air purifier negative ion generator [29]" at the plates, a negative saturation voltage was observed at the output of our two-stage amplifier. This translates to the plates sourcing a current when ions hit said plates. This is the opposite of the expectation: it behaves as a current source. A possible explanation follows:
The negative ions were incident on the plates, and in doing so delivered negative charge to the plates. This creates a small, non-negligible negative potential on the plates. This voltage is lower than that at the inverting terminal of the opamp - and the opamp supplies power at the output to maintain this voltage. Then Ohm's law, $V = I \cdot R$, where R is the resistance of the wire connecting one plate to the inverting input of the opamp, dictates a current I must flow towards the plates. The transimpedance amplifier then outputs a positive voltage of $I \cdot R_g$, which was inverted in their [28] second stage, producing the unexpected negative voltage at the output.
For this reason, the circuit layout was modified to implement a non-inverting second stage, as shown in Figure 9b. Here V_{plate} is the voltage put over the ion sensor plates, which are drawn as a capacitor

in the schematic. R_g is the gain element of the first stage, and has a resistance of $1 \cdot 10^9\Omega$. The $100k\Omega$ variable resistor was implemented with a potentiometer to allow for slight gain control. The $3pF$ capacitor in parallel with R_g functions as a low pass filter for the amplifier. However, due to time constraints and lesser priority of this sensor as a trade-off requirement, calibration of this sensor has been postponed.

5.4 Ozone sensors

As described in subsection 1.2, ozone is an effective disinfection agent. However, excessively high concentrations can also be damaging to the seeds [30]. Therefore monitoring the ozone concentration is essential to our disinfection system. Due to our air circulation method, we expect a wide range of ozone concentrations. For this reason, we have implemented two sensors: a coarse resolution sensor [31] with range from 10ppm to 1000ppm, and a fine resolution sensor [32] with a range between 0ppm and 10ppm. Images of these sensors are found in Figure 10.

(a) Ozone2Click ozone sensor, rated from 10-1000ppm. Image from product datasheet [31].

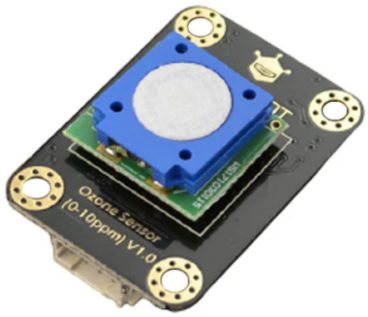

(b) Gravity IIC Ozone Sensor, rated from 0-10ppm. Image from [33].

Figure 10: Ozone sensors used in the fluidized bed.

The coarse resolution sensor, the Ozone2click, operates via the Serial Peripheral Interface (SPI), and returns a voltage value. The fine resolution sensor, the Gravity IIC Ozone sensor, communicates via the Inter-Integrated Circuit (I2C) protocol. Both protocols are commonly supported by commercial microcontrollers. Together with their measurement ranges, this ease of use supports our choice of these sensors.

For calibration of the ozone sensors, the setup in Appendix B was constructed (see Figure 21. Some experimental electrodes based on the fractal design of dr. Luutzen Wymenga were attached to a 50Hz 15kV lab voltage source, and produced the ozone. A lab-grade ozone meter with measurement range from 0ppm to 5ppm was added in the setup for reference to confirm the calibration of the Gravity IIC Ozone sensor (which claimed to be pre-calibrated [32]). The data were collected using a Raspberry Pi Pico and the software PuTTY.

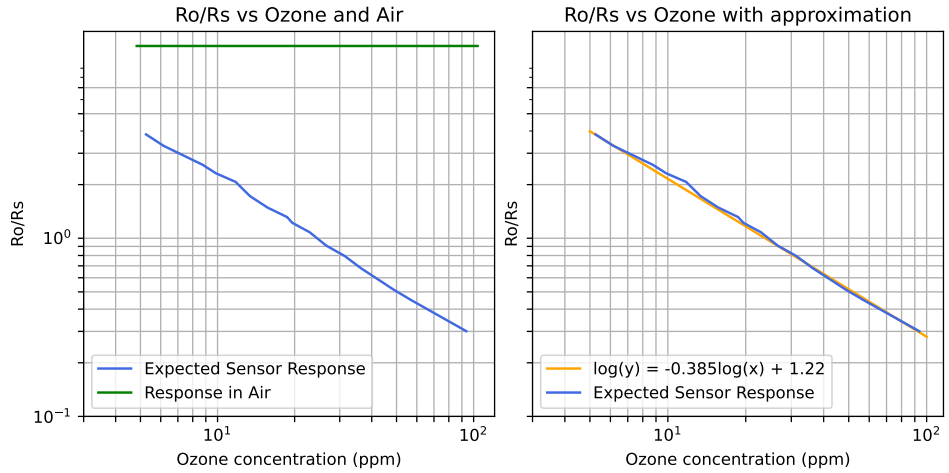

Figure 11: Expected Ozone Sensor Response from [31]

The Ozone2click is a component that supports the operation of the MQ131 Semiconductor Sensor [31] [34]. This sensor operates based on a variable resistor component made out of SnO_2, whose resistance increases with ozone concentration [34]. The ozone concentration is measured using the ratio of a reference point R_0, the resistance of the sensor in 50ppm Ozone, and the current sensor resistance R_s, as depicted in the left hand side of Figure 11. The curve data points were extracted using the software Engauge Digitizer, and Python code was used to create the pseudo-linear approximation depicted in the right hand side of Figure 11. The approximation uses x as the ozone concentration in parts per million, and y as the measurement ratio.
Unfortunately, no calibrated sensor that could measure 50ppm ozone was available. Thus R_0 was then approximated by measuring the ratio of $R_0/R_s = 12$, when the sensor was in normal air, a as reference (also plotted in the left hand side of Figure 11. The value for R_s is described by Equation 6 [34]:

$$R_s = (\frac{V_c}{V_{RL}} - 1) \cdot R_L \tag{6}$$

Where $V_c = 5V$ is the supply voltage, V_{RL} is the measured output voltage, and $R_L = 7500\Omega$ is the value of a variable resistor. In air, $\frac{R_0}{R_s} = 12$, and $V_s = 2V$, so R_0 was found to be $135k\Omega$. Then, rewriting the pseudo-linear approximation to be $x = 10^{\frac{log(y)-1.22}{0.385}}$ where $y = \frac{R_0}{R_s}$, the measured voltage data can be converted to ozone concentration.

Using the setup described above, ozone was generated for roughly eight minutes. A that point, the ozone concentration did not rise significantly any longer, either due to leakage from the tank, or because there was not enough oxygen left near the electrode to create plasma. Then the power on the electrode was turned off, and the sensors were left in the tank while the ozone concentration dropped for roughly the same time. These time-based measurements are depicted in Figure 12.

The code used for plotting is shown in Appendix C. In the plots of Figure 12, a definite mismatch between the Ozone2click and Gravity IIC Ozone sensor is seen. Despite the large voltage swing, negligible concentration was measured with the current assumption of R_0 for the Ozone2click sensor. The third plot in Figure 12 is a closeup of the ozone concentration measured by the Ozone2click, showing a maximum concentration of 0.55ppm. The difference in concentration measurements is surprising, especially when the data from the lab measurement device is taken into account. This highest concentration in the lab setup was 0.47ppm. The result of calibration is then that the Ozone2click is roughly correctly calibrated, whilst the 'already calibrated' Gravity IIC Ozone sensor is wildly off.

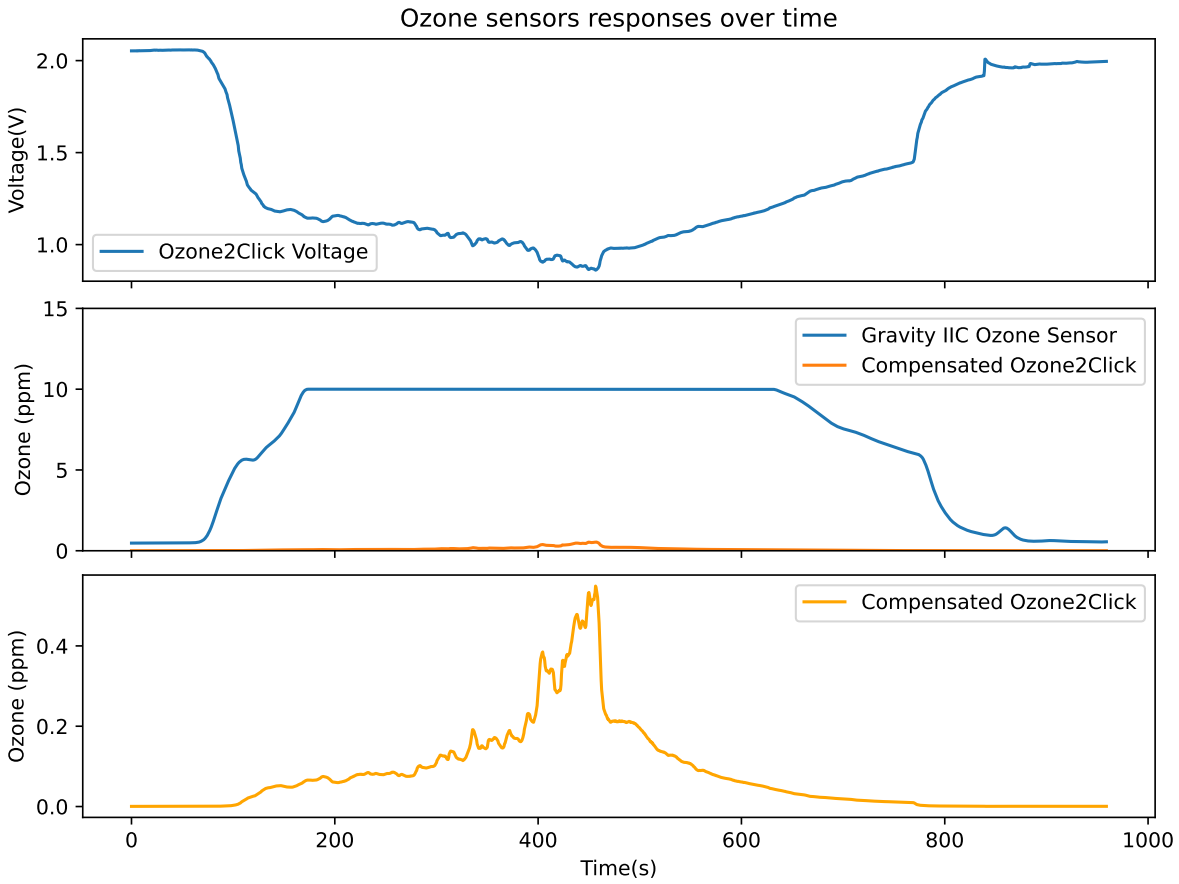

Figure 12: Calibration Response of ozone sensors

5.5 Temperature and humidity sensor

Figure 13: AM2315C combined temperature and humidity sensor. source: [35]

The next sensor that was implemented in the system is a combined humidity and temperature sensor, depicted in Figure 13. As described in [36], the relative humidity of the air used during plasma creation influences the ratio of ozone and OH radicals. Additionally, the required voltage increases slightly with humidity [36]. Humidity has also been shown to negatively affect electrode deterioration as well as plasma generation [37]. Due to these influences on our plasma chamber, our design implements a temperature-humidity sensor, namely the AM2315C [35]. This sensor has a sensitivity range between 10% and 90% relative humidity, and can communicate via I2C protocol. Since this range is larger than that used in [36], this range is sufficiently large for our purpose. The sensor was successfully implemented using the I2C bus of a microcontroller.

5.6 Conclusions

To monitor the performance of the fluidized bed setup, several sensors were implemented. These include a mass flow sensor, an ion density sensor, ozone sensors, and a combined temperature and humidity sensor. Argumentation was provided as to the choice of sensors made. Sensor calibration was done for the ozone and flow sensors, and a rough construction of an ion sensor was made.

6 Prototype Integration

6.1 Introduction

In this section, the total integration of the sensor and fluidized bed into a single system will be discussed. The sensors described in section 5 were integrated into a single measurement system, with an easy readout method using a set of small displays. Finally, the displays and the total of the readout electronics were mounted in a 3D printed case designed in CAD. In this section, the integration and powering of the electronics will be discussed, after which the sensor and electronics mounting and the considerations behind this will be mentioned.

6.2 Electronics

6.2.1 Readout implementation

The readout of sensor values was implemented using the microcontroller board Raspberry Pi Pico. This microcontroller is easily programmable using C++ code and the Arduino IDE, and is powered by a 5 volt supply. The microcontroller was chosen since it provided a complete package for all desired analog and digital inputs: the board contains three analog inputs, two I2C buses, an SPI interface, and the ability to generate PWM signals. These features are ideal, because of the analog outputs of the ion density meter, air flow meter, and also for a potentiometer for fan motor control. Additionally, the coarse ozone sensor communicates via SPI, and the thermo-humidity sensor, fine ozone sensor, and OLED display boards communicate via I2C. The two used displays have the same I2C address, which is why the two different buses are ideal. The Raspberry Pi Pico converts the sensor data to usable units, according to factory or self-performed calibration and displays it on the screens. The complete circuitry providing power and signal paths between sensors and microcontroller was constructed on a prototype circuit board, with removable connectors for connection of displays and sensors (see Figure 14). The circuitry diagram (Figure 22) is found in appendix C.

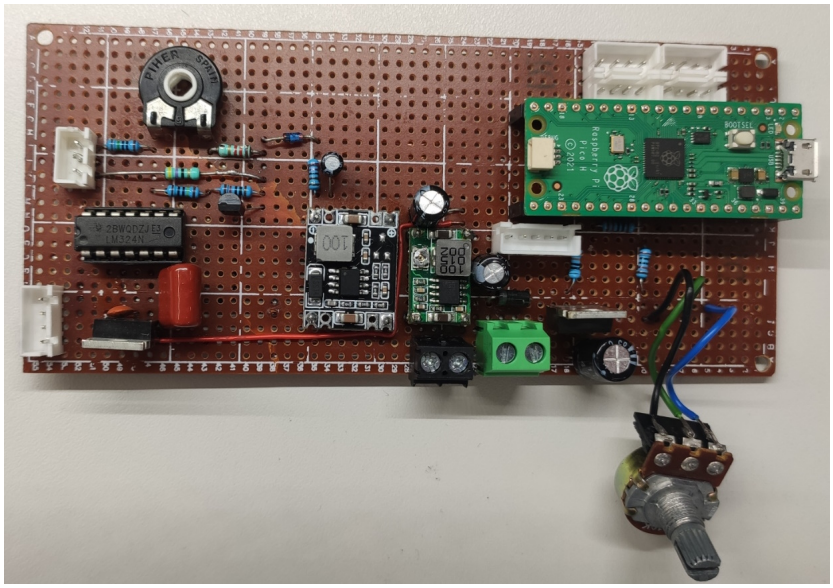

Figure 14: The complete sensor board, constructed on a prototype circuit board.

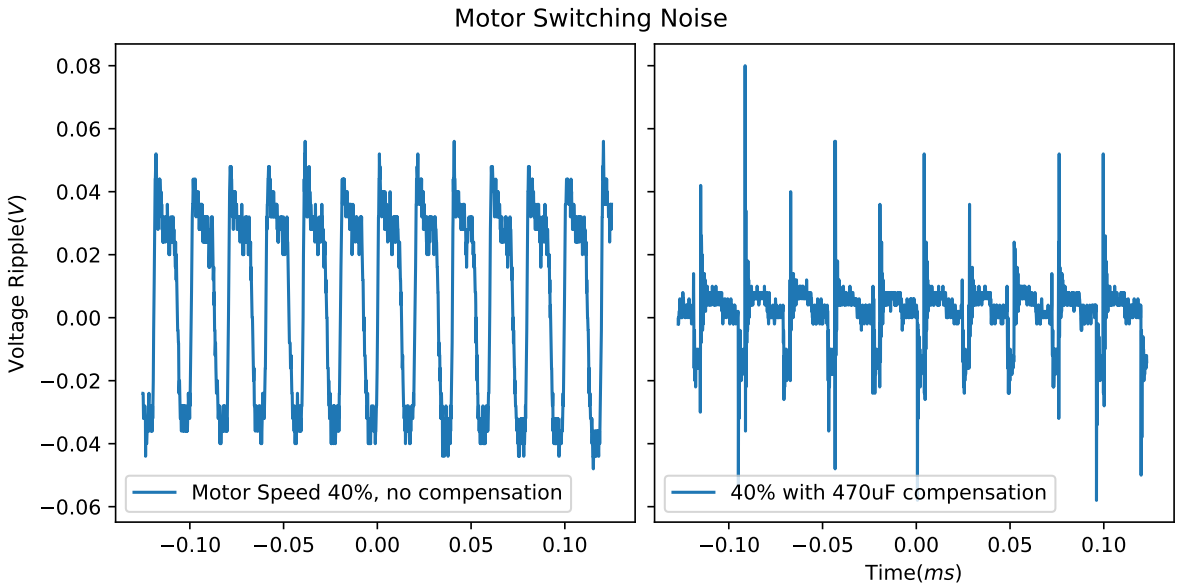

Figure 15: Switching noise on the 12V supply before and after compensation at 40% motor speed.

6.2.2 Powering of fluidized bed and sensor electronics

The fluidized bed was powered using a 12V 10A power supply. The fluidized bed motors were powered using this 12V supply, controlled by a PWM signal, which in turn controls a logic level MOSFET that switches the motors, allowing for precise power control to the motors. Some noise was observed on the power rail due to the PWM switching of the motors, and is depicted in Figure 15 and in Appendix A. This was measured with a standard oscilloscope, using a 1x attenuation calibrated oscilloscope probe with coaxial cable. Special care was taken to remove this noise caused by the rapid switching of the fans to limit the effects of the noise on the analog measurements. This was done by adding a flyback diode across the terminals of the fans, and using a decoupling capacitor from the negative terminal of the fan to ground after switching. Addition of these components resulted in a drastic reduction in noise, benefiting the analog sensors. To further reduce noise, the wind speed sensor was powered by a linear voltage regulator with a set of decoupling capacitors for better noise performance.

The lower power digital components which are not as sensitive to noise were powered by a DC-DC buck converter, for efficiency reasons. The ozone sensors contain a sensing mechanism involving a heater, requiring larger currents, for which linear regulators are less suitable.

6.3 Case design and sensor mounting

After the electronics were integrated, they were mounted inside a case that allows for easy readout of the sensors. A case was designed in CAD, providing a sturdy housing for the electronics and displays (as seen in Figure 16a). The housing also contains easy access to a potentiometer used for motor speed control. In addition to the electronics, the sensors were mounted inside the fluidized bed (as seen in Figure 16b). Special care was taken to the positioning of the sensors. Following manufacturer guidelines, the ozone sensors should not be located inside a strong draft. Therefore, the ozone sensors were inserted inside the side walls of the fluidized bed, away from the exhaust exits. This was done to prevent direct air flow across the sensors. The combined temperature and humidity sensor was mounted close to the other sensors. The location of the sensor was reasoned to not be of high importance, since the high flow rate of the fluidized bed was assumed to create constant conditions. The flow sensor was

(a) Display and electronic housing.

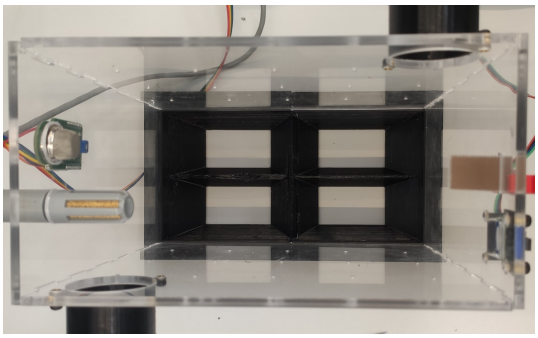

(b) Mounting of sensors inside the fluidized bed, as seen from above.

Figure 16: Mounting solution of sensors and electronics.

placed inside one of the re-circulation pipes, since the range of air speeds is higher within the narrow tube as compared to the inside of the fluidized bed, which caused a larger range of air speeds. Finally, the ion sensor was placed above the electrodes inside the air stream, since the ion sensor proved to provide the best results when placed directly in an ion stream.

6.4 Conclusions

The fluidized bed and sensor system integration were discussed in this chapter. A readout circuit was constructed with a Raspberry Pi Pico, several DC-DC power converters were used, as well as some switching noise compensation. The sensors were mounted according to manufacturer recommendations and functional requirements, and the readout circuitry was placed in a housing on the side.

7 Testing

7.1 Introduction

This section describes some tests that were executed to validate the design functionality. The lab setup is shown, the some of the data is displayed, and then also discussed.

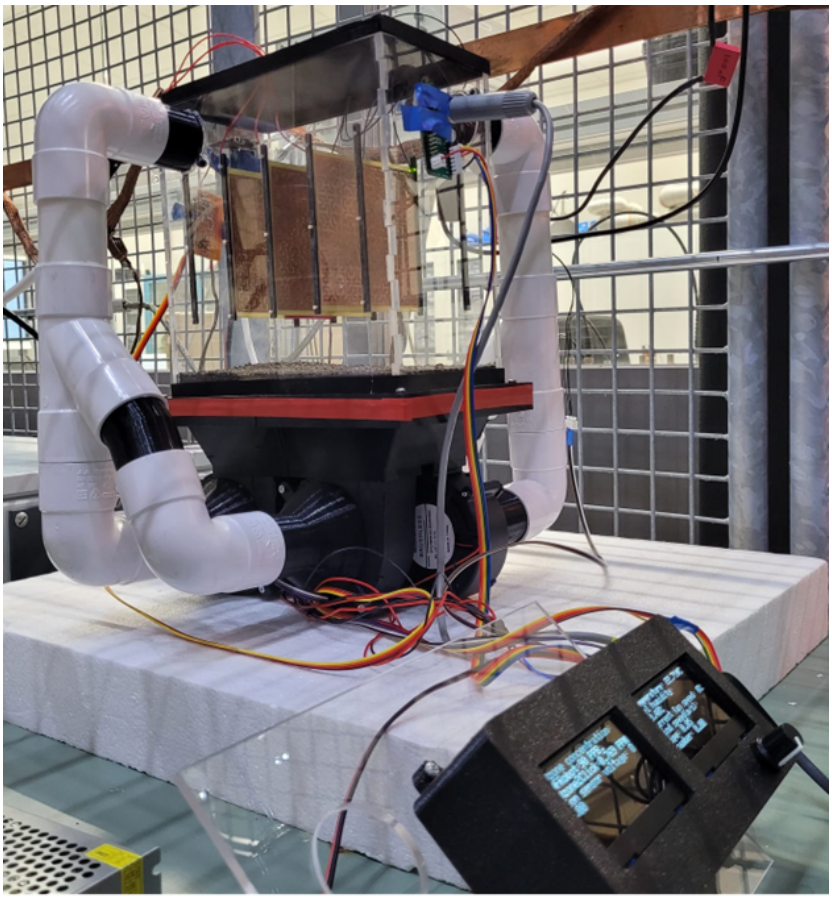

(a) Lab setup with three electrodes.

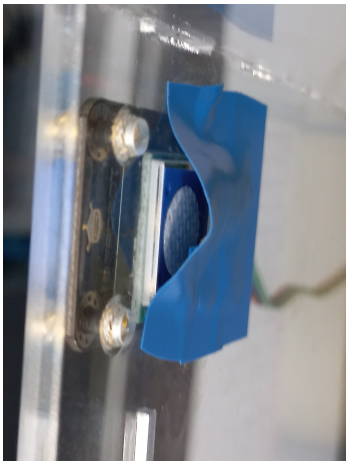

(b) Airflow shielding DFRobot IIC ozone sensor

Figure 17: Mounting solution of sensors and electronics.

7.2 Lab setup

The lab setup used to test our design is shown in Figure 17a. The figure shows the bubbling configuration, with three electrodes in the middle (however, in the conducted tests only one electrode was used, as will be discussed later on). These were then connected to a 50Hz variable AC high voltage source with overcurrent protection. The sensor readout was connected via USB cable to a laptop for the purpose of data logging (executed with PuTTY).

7.3 Plasma Breakdown

The next observation made was that of arcing at around 12kV. During the experiment, the voltage was gradually increased with the purpose of reaching 18-20kV. However, during the raising of the

voltage, the overcurrent protection feature of the source went into effect. This consistently occurred around the 12kV point. This voltage was lower than the experimentally determined voltage that was required [6] for efficient plasma production. It was found that the acrylic side walls of the chamber helped form arcs. To avoid this arcing, the 15-minute seed treatment trial run was conducted with only one electrode rotated by 90 degrees as opposed to the setup shown in Figure 17a. The electrode was positioned such that it did not touch the sides of the chamber, to prevent arcing. Only one electrode was used due to spacial restrictions of the configuration.

7.4 Ozone concentration

The next observation made was that the ozone concentration did not rise over time when there was airflow, as seen inFigure 18. The measurements should be interpreted in a qualitative manner, since they are taken with the DFRobot sensor. Several possible explanations are presented in section 8.

7.5 Treatment Results

As mentioned above, some of the seeds were treated in the chamber for a period of fifteen minutes. The seeds available were non-contaminated. A large sample of these treated seeds were sent to the labs at Bejo Zaden for in-depth analysis, and a few were placed locally in Petri dishes. Figure 19 shows the growth of the treated (right) and non-treated (left) seeds. Each box contained 150 seeds. The germination rates, a desirable side effect of ozone treatment, was found to be 94% and 91% respectively. These rates are comparable, and insufficient evidence for decisive conclusions.

7.6 Conclusions

In this section the testing of the setup was discussed. Inside the setup, increased ozone concentrations were observed, but the airflow inside the setup during fluidization caused the ozone concentration to saturate at low values. The germination rates of the seeds was examined before and after treatment. Our sample proved to be of healthy seeds, and similar germination rates of 91% before treatment and 94% with treatment were observed.

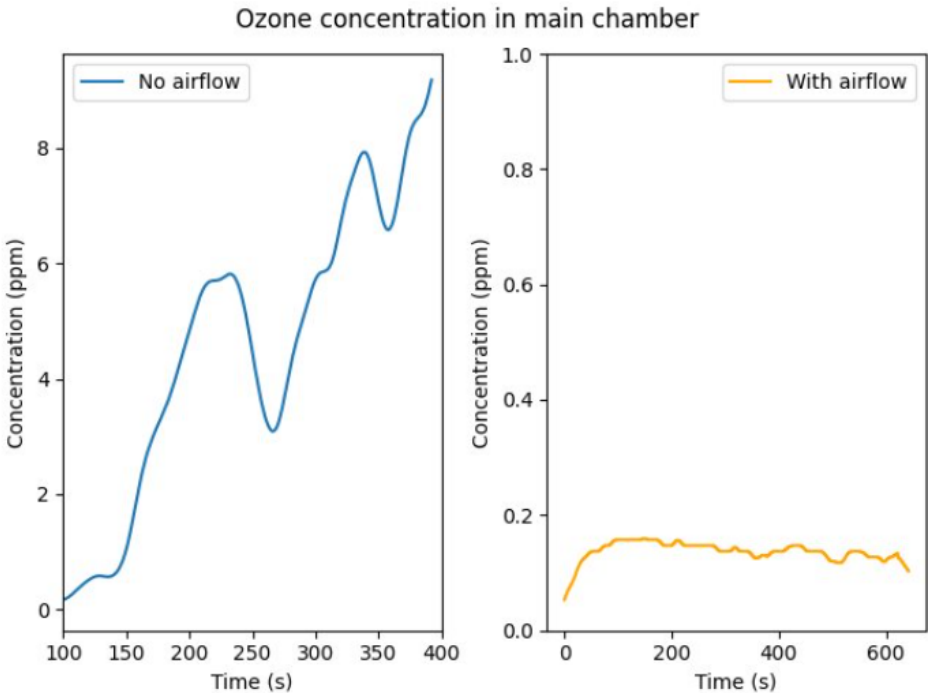

Figure 18: Ozone concentration in main chamber with and without airflow.

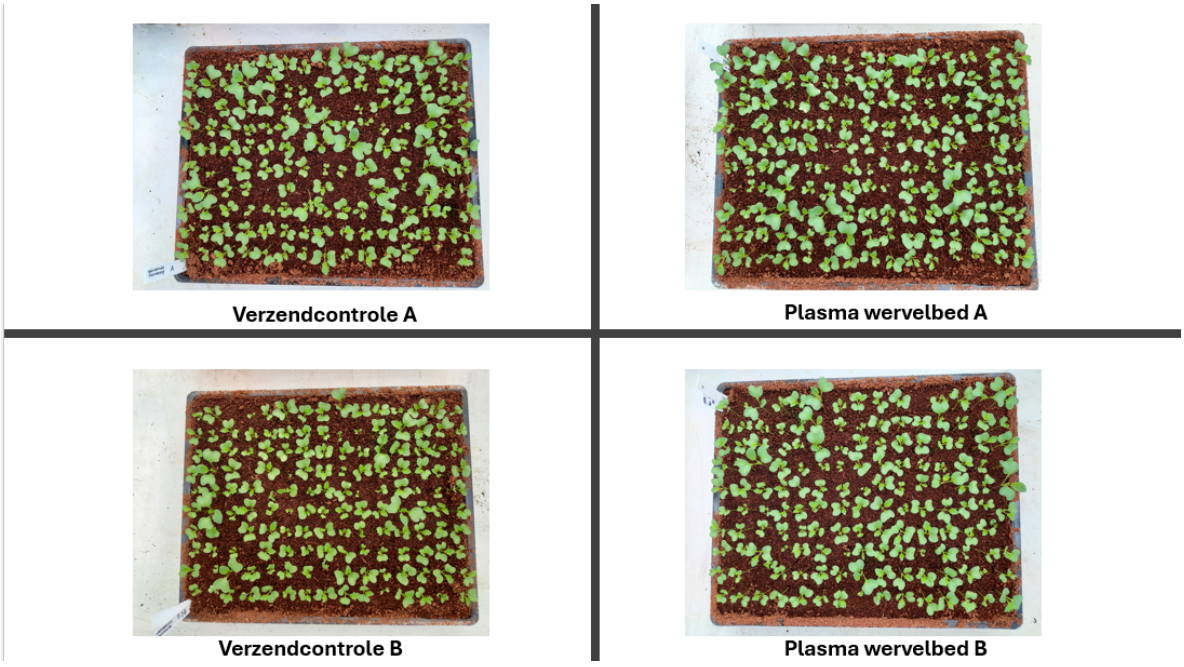

Figure 19: Germination rate test results.

8 Discussion

In this section the results of the design are discussed.

8.1 Fluidized and Spouted Bed

The fluidized bed main structure is sturdy, and was tested to be functional with quantities up to 700ml of seeds in both a bubbling and a spouted bed. The fans provide sufficient power to allow for fluidization, and the fluidization mixes the seeds well overall. In the bubbling bed, there appeared deadzones in certain places around the edges, due to the behaviour of the radial fans. The effects were more pronounced with larger quantities of seeds due to the increased pressure drop through the bed. Thus, for higher quantities of seeds, the disinfection may prove to be worse. For larger bed heights, special attention must be given to providing a high and constant pressure air supply.

The spouted bed provided good results for lower quantities of seeds, but mixing proved to become worse for increasing quantities of seeds in the setup. The spouting provided large vertical movement of the seeds, but not as much horizontal movement. The setup needs to run for longer to provide adequate mixing. However, the larger vertical movement of seeds ensure close contact to the plasma units in the chamber. This may have positive effects on disinfection. Additionally, spouting was easier to initiate and sustain, requiring lower air flow and speed, making it a more power efficient option.

8.2 Sensors

Regarding sensors, two ozone sensors, one thermo-humidity sensor, a flow sensor, and an ion sensor were implemented. The high concentration Ozone2click sensor was calibrated using plots from its respective datasheets to a commercial ozone sensor. The low concentration Gravity IIC Ozone sensor showed a much more sensitive response than the lab sensor. It is possible that this sensor is also sensitive to other molecules that are created by plasma, such as hydroxl, H_2O_2, or NO_x species. Additionally, as seen in Figure 12, the response to changing ozone concentration of this sensor was slower than that of the Ozone2click, indicating a memory behaviour.

The mass flow sensor functionality was slightly different than described in its application note [27]. Its output voltages were slightly lower, which is likely caused by the lower power supply rail of 9 volts via the linear voltage regulator. However, the test measurements followed the calibration curve closely across the entire range.

The ion sensor has been roughly constructed, and has yet to be properly calibrated. Its behavior is rather binary: The sensor either reads nothing, or saturates quite quickly. This indicates an extremely high sensitivity. It is possible that the ions released from the commercial ion generator were not evenly dispersed in the air, thus hitting the sensor in batches large enough to saturate it. As the ion source only emitted negative ions, its behaviour is unknown for positive ions.

8.3 Final Test Results Discussion

Finally, a test was conducted with the entire setup. During fluidization, the ozone concentration in the setup saturated at a significantly lower value than without the fluidization turned on. While the exact reason is unknown, there are some possible explanations.

The first possible explanation is that the ozone sensors are sensitive to airflow, due to their heating element [32]. Some tape was added to shield the sensor from airflow, as seen in Figure 17b. However, this still may affect the measurements slightly.

Another factor to consider is that the ozone recombination rate increases with airflow [38]. This is not considered to be sufficient to explain our results, as at our air speed the recombination rate of ozone is in the order of hours, whilst our air recirculates roughly every half second. There may still be some unaccounted pressure buildup in the corners of the pipes that may affect ozone recombination rate, but this is assumed not to be significant on our scale.

The final factor to consider is ozone loss by chemical reactions with the materials inside the setup and the environment. Since our construction is made of ozone-resistant materials, this would infer that the seeds act as a filter for the ozone, and that our treatment method is effective. Unfortunately no ozone was generated without seeds to validate this assumption, due to constraints with testing facility access. This would have been instrumental to conclusive results.

9 Conclusions and recommendations

In this thesis, the design an implementation of a fluidized bed with sensors for the purpose of seed disinfection was realized. Both a bubbling and spouting fluidized bed were constructed in CAD, with the bubbling bed having more consistent performance than the spouting configuration. Furthermore, a series of sensors and the readout system were implemented into a complete readout package with displays. A mass flow sensor, a set of ozone sensors, a temperature and humidity sensor were implemented in the system, providing an accurate measure of the disinfecting conditions inside the fluidized bed. Additionally, a first version of a compact ion sensor was constructed, which can be developed further. The sensors were implemented in a fluidized bed, making the system ready for testing disinfection performance with seeds. A first test was done using the system on healthy, uninfected seeds. These tests, where sets of 300 seeds were tested, showed an increase in germination rate from 91 to 94 percent.

There are several aspects that further research is recommended for. Regarding fluidized bed construction, there are unexplored topologies of fluidized beds in plasma disinfection that are also promising, like the circulating fluidized bed and vibrating fluidized bed.

Next, there are several considerations regarding the sensor system. For instance the ion sensor, which requires rigorous testing and tuning. Recommended is to place it with an ion source in an enclosed chamber with a commercial, lab grade ion sensor. Then the ion source should be turned on, and concentration of ions in the chamber allowed to increase. If possible to allow the concentration to rise uniformly this should be implemented, to rule out the speculated batch behaviour.

Another valuable addition of the system would be data recording. The system has data logging capabilities via USB, so a valuable addition to the system would be to add data logging functionality. This would allow for automatic tracking of conditions during the disinfection process. Data logging could also be easily implemented using wireless communication, since the used Raspberry Pi Pico microcontroller can be replaced for a wifi-enabled version, which could provide safe distance and isolation for high voltage testing with plasma electrodes.

Another suggested addition to the system is the implementation of a control system that feeds back the measured ozone concentration, which would allow for the possibility to set a target ozone concentration. This would be beneficial, since high concentrations of ozone and reactive species may react with the materials the fluidization setup is made of, and would contribute to a shorter lifespan. Additionally, treatments can be made more energy efficient in this way by switching the plasma modules off when a desired concentration is reached.

As future work on the project, the created system should be tested using an increased number of DBD plasma electrodes [6], instead of the single electrode that was used in the experiment. Additionally, a higher frequency power supply created for seed disinfection by [5] should be tested to create elevated ozone concentrations. Finally, the seeds require testing for microbial activity to validate the disinfection performance of the setup.

Appendix A

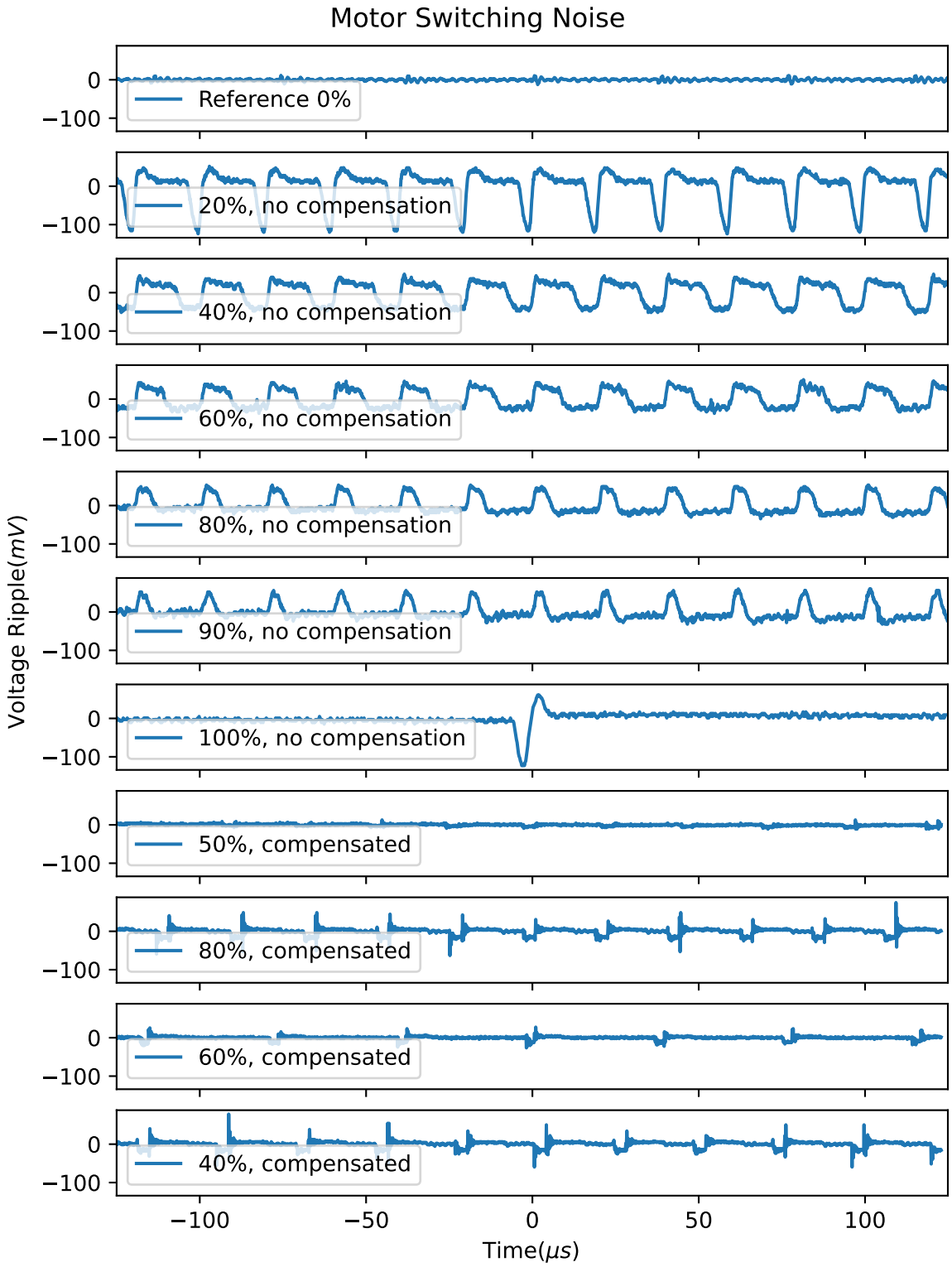

Figure 20: Switching noise on power rail

Appendix B

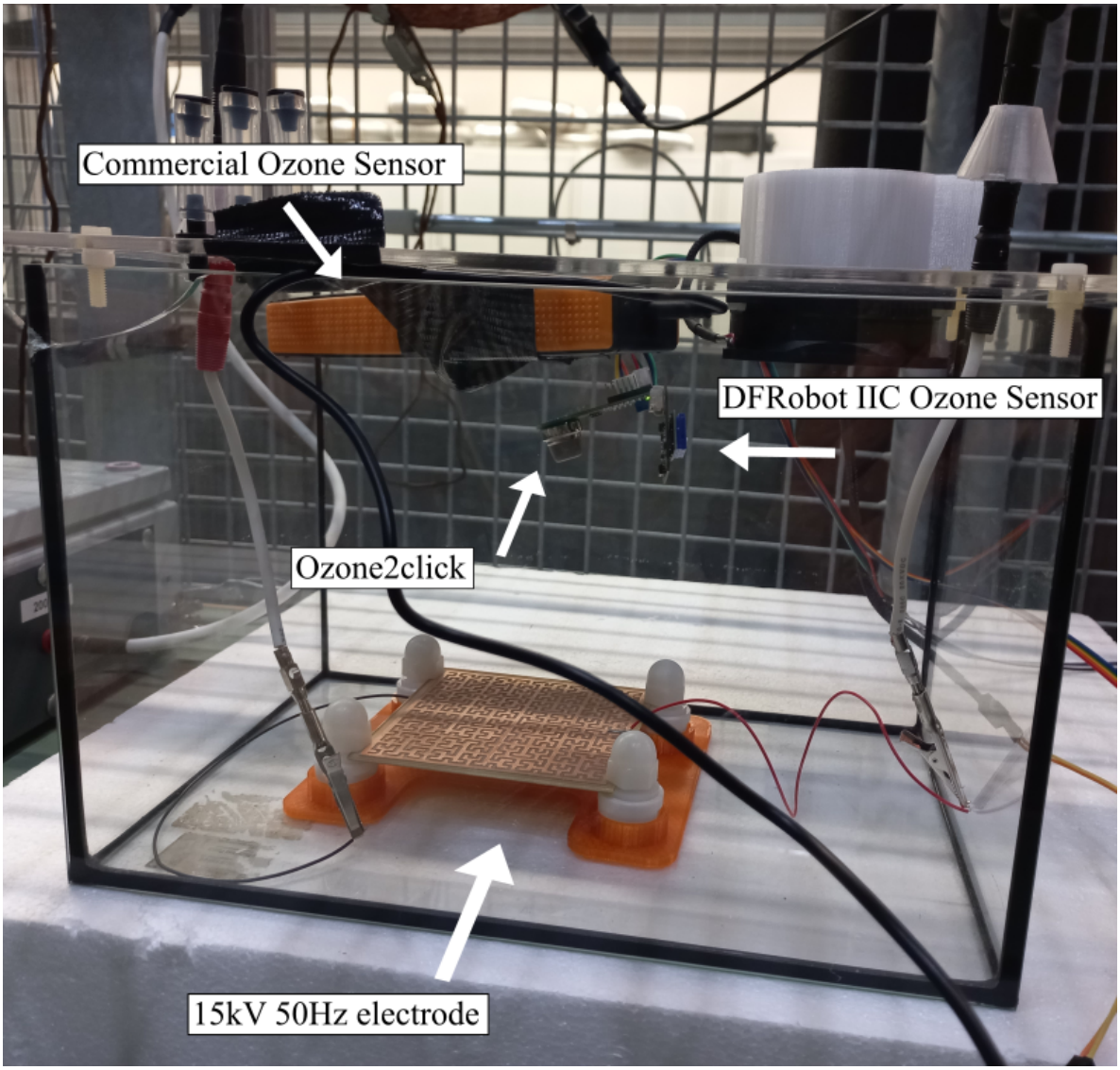

Figure 21: Ozone sensor calibration testing setup

Appendix C

In this appendix, used code for making plots and doing calculations is added.

```
import numpy as np
import matplotlib.pyplot as plt
import csv

def Ozone_finder(Rs, Ro=135000):
  a = -0.385
  b = 1.22
  Oz = 10**((np.log(Ro/Rs)-b)/a)
  return Oz

def Rs_finder(Vm):
  RL=7500
  Vc = 5
  return (Vc/Vm-1)*RL

fig, ax = plt.subplots(3, 1, figsize=(8,6),constrained_layout=True, sharey=False,
    sharex=True)

Oz_big = np.zeros(1919)
big = np.zeros(1919)
small = np.zeros(1919)
time = np.zeros(1919)
with open('ozone_data.log', mode ='r')as file:
  csvFile = csv.reader(file)
  i = 0
  for lines in csvFile:
    big[i] = lines[0]
    Oz_big[i] = Ozone_finder(Rs_finder(big[i]))
    small[i] = lines[1]
    time[i] = 0.5*i
    i = i + 1
  print(i)
  print(max(Oz_big))

ax[0].plot(time,big, label="Ozone2Click Voltage")
ax[1].plot(time,small/1000, label="Gravity IIC Ozone Sensor") #factor 1000 is because
    sensor measures ppb
ax[1].plot(time,Oz_big,label="Compensated Ozone2Click")
ax[2].plot(time,Oz_big,label=f"Compensated Ozone2Click", color='orange')
ax[0].legend()
ax[1].legend()
ax[2].legend()
ax[1].set_ylim((0,15))
plt.xlabel("Time(s)")
ax[0].set_ylabel("Voltage(V)")
ax[1].set_ylabel("Ozone (ppm)")
ax[2].set_ylabel("Ozone (ppm)")
ax[0].set_title("Ozone sensors responses over time")
plt.show()
# plt.savefig("big_ozone_estimate.pdf")
```

Appendix D

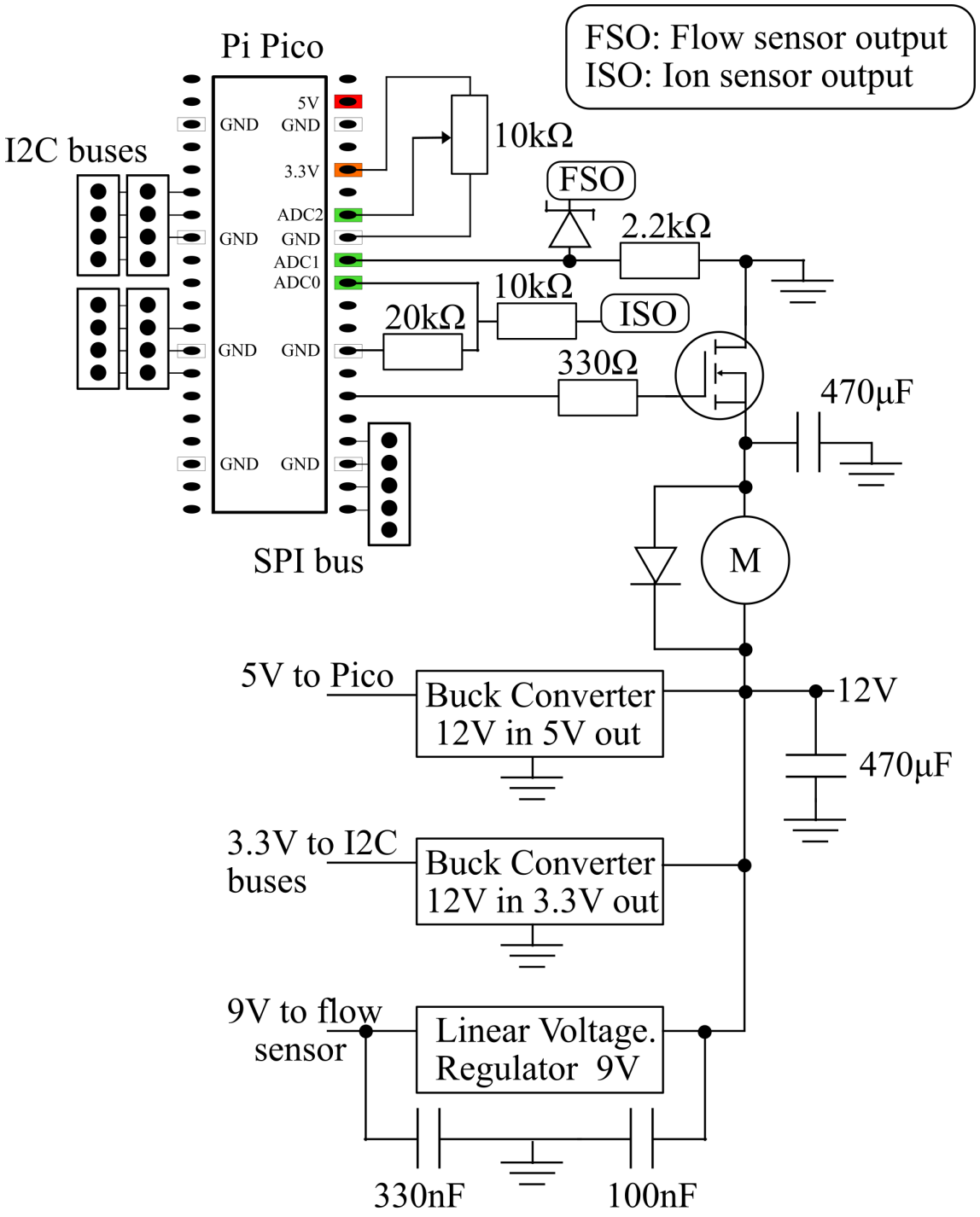

Figure 22: Sensor Board Schematic

References

[1] S. Pedrini, D. J. Merritt, J. Stevens, and K. Dixon, "Seed coating: science or marketing spin?" *Trends in plant science*, vol. 22, no. 2, pp. 106–116, 2017.

[2] G. S. Gilbert, A. Diaz, and H. A. Bregoff, "Seed disinfestation practices to control seed-borne fungi and bacteria in home production of sprouts," *Foods*, vol. 12, no. 4, p. 747, 2023.

[3] D. Dobrynin, G. Friedman, A. Fridman, and A. Fridman, "Photons and particles emitted from cold atmospheric-pressure plasma inactivate bacteria and biomolecules independently and synergistically," *Plasma Processes and Polymers*, vol. 10, no. 7, pp. 636–646, 2013, accessed: 2024-06-09. [Online]. Available: https://www.researchgate.net/publication/257074627_Photons_and_particles_emitted_from_cold_atmospheric-pressure_plasma_inactivate_bacteria_and_biomolecules_independently_and_synergistically

[4] J. Ehlbeck, U. Schnabel, M. Polak, J. Winter, T. V. Woedtke, and K.-D. Weltmann, "Cold plasma: background, applications, and current trends," *Psycho-social Medicine*, 2017, accessed: 2024-06-09. [Online]. Available: https://www.researchgate.net/publication/318925675_Cold_plasma_background_applications_and_current_trends

[5] Z. Hayaty and B. Salar, "High voltage generator for eco-friendly plasma-disinfection of seeds," *unpublished BSc Thesis Delft University of Technology*, 2024.

[6] C. Buitink and J. Lohman, "Plasma dbd electrodes plasma fluidized bed," *unpublished BSc Thesis Delft University of Technology*, 2024.

[7] H. Ding, T.-J. Fu, and M. A. Smith, "Microbial contamination in sprouts: how effective is seed disinfection treatment?" *Journal of Food Science*, vol. 78, no. 4, pp. R495–R501, 2013.

[8] J. Mravlje, M. Regvar, and K. Vogel-Mikuš, "Development of cold plasma technologies for surface decontamination of seed fungal pathogens: Present status and perspectives," *Journal of Fungi*, vol. 7, no. 8, p. 650, 2021.

[9] D. Pańka, M. Jeske, A. Łukanowski, A. Baturo-Cieśniewska, P. Prus, M. Maitah, K. Maitah, K. Malec, D. Rymarz, J. d. D. Muhire *et al.*, "Can cold plasma be used for boosting plant growth and plant protection in sustainable plant production?" *Agronomy*, vol. 12, no. 4, p. 841, 2022.

[10] F. Ciccarese, N. Sasanelli, A. Ciccarese, T. Ziadi, and L. Mancini, "Seed disinfestation by ozone treatments," in *Proceedings of the IOA Conference and Exhibition*, 2007, pp. 29–31.

[11] M.-H. Kang, M. Veerana, S. Eom, H.-S. Uhm, S. Ryu, and G. Park, "Plasma mediated disinfection of rice seeds in water and air," *Journal of Physics D: Applied Physics*, vol. 53, no. 21, p. 214001, 3 2020. [Online]. Available: https://dx.doi.org/10.1088/1361-6463/ab79de

[12] M. Świecimska, M. Tulik, B. Šerá, P. Golińska, J. Tomeková, V. Medvecká, H. Bujdáková, T. Oszako, A. Zahoranová, and M. Šerý, "Non-thermal plasma can be used in disinfection of scots pine (pinus sylvestris l.) seeds infected with fusarium oxysporum," *Forests*, vol. 11, no. 8, 2020. [Online]. Available: https://www.mdpi.com/1999-4907/11/8/837

[13] B. G. Dasan, I. H. Boyaci, and M. Mutlu, "Nonthermal plasma treatment of aspergillus spp. spores on hazelnuts in an atmospheric pressure fluidized bed plasma system: Impact of process parameters and surveillance of the residual viability of spores," *Journal of Food Engineering*, vol. 196, pp. 139–149, 2017.

[14] M. Măgureanu, R. Sîrbu, D. Dorbin, and M. Gîdea, "Stimulation of the germination and early growth of tomato seeds by non-thermal plasma," *Plasma Chemistry and Plasma Processing*, vol. 38, pp. 989–1001, 2018. [Online]. Available: https://doi.org/10.1007/s11090-018-9916-0

[15] C. Du, R. Qiu, and J. Ruan, *Plasma Fluidized Bed*. Springer, 5 2018.

[16] B. Ulejczyk, L. Karpiński, M. Scholz, M. A. Ekwińska, Z. Rymuza, T. Opalińska, E. A. Żukowska, and K. Schmidt-Szałowski, "Deposition of silicon oxide film from tetraethoxysilane using a pulsed dielectric barrier discharge," *Czechoslovak Journal of Physics*, 2006.

[17] G. Forsberg, S. Andersson, and L. Johnsson, "Evaluation of hot, humid air seed treatment in thin layers and fluidized beds for seed pathogen sanitation/bewertung der saatgutbehandlung mit heißer, feuchter luft und in einer verwirbelungskammer zur eliminierung von samenbürtigen pathogenen," *Zeitschrift für Pflanzenkrankheiten und Pflanzenschutz/Journal of Plant Diseases and Protection*, pp. 357–370, 2002.

[18] D. Geldart, "Types of gas fluidization," *Powder technology*, vol. 7, no. 5, pp. 285–292, 1973.

[19] R. Cocco, S. R. Karri, T. Knowlton *et al.*, "Introduction to fluidization," *Chem. Eng. Prog*, vol. 110, no. 11, pp. 21–29, 2014.

[20] S. Safarian, R. Unnbórsson, and C. Richter, "A review of biomass gasification modelling," *Renewable and Sustainable Energy Reviews*, vol. 110, p. 378–391, Aug. 2019.

[21] V. S. Sutkar, N. G. Deen, and J. Kuipers, "Spout fluidized beds: Recent advances in experimental and numerical studies," *Chemical Engineering Science*, vol. 86, pp. 124–136, 2013, 5th International Granulation Workshop. [Online]. Available: https://www.sciencedirect.com/science/article/pii/S0009250912003715

[22] C. Wen and Y. Yu, "A generalized method for predicting the minimum fluidization velocity," *AIChE journal*, vol. 12, no. 3, pp. 610–612, 1966.

[23] J. Richardson and M. d. S. Jerónimo, "Velocity-voidage relations for sedimentation and fluidisation," *Chemical Engineering Science*, vol. 34, no. 12, pp. 1419–1422, 1979.

[24] *DC Blower BFB1012VH-A*, Delta Electronics, 2 2005.

[25] W. Jittanit, G. Srzednicki, and R. H. Driscoll, "Comparison between fluidized bed and spouted bed drying for seeds," *Drying Technology*, vol. 31, no. 1, pp. 52–56, 2013.

[26] Innovative Sensor Technology, "Thermal mass flow sensor," FS7.A.1L.195 datasheet.

[27] ——, "Thermal mass flow sensor - application note," aFFS7_E2.3.0 application note.

[28] O. Anttalainen, E. Lattouf, T. Kotiaho, and G. Eiceman, "Ion density of positive and negative ions at ambient pressure in air at 12–136 mm from 4.9 kv soft x-ray source," *Review of scientific instruments*, vol. 92, no. 5, 2021.

[29] https://www.amazon.nl/dp/B07JMJ6FCP?ref=ppx_yo2ov_dt_b_product_details&th=.

[30] R. Pandiselvam, V. Mayookha, A. Kothakota, L. Sharmila, S. Ramesh, C. Bharathi, K. Gomathy, and V. Srikanth, "Impact of ozone treatment on seed germination–a systematic review," *Ozone: Science & Engineering*, vol. 42, no. 4, pp. 331–346, 2020.

[31] MikroElectronica, "Ozone 2 click," PID: MIKROE-2767 datasheet.

[32] DFRobot, "Gravity IIC Ozone Sensor (0-10ppm) SKU SEN032," SEN0321 datasheet.

[33] Apr 2020. [Online]. Available: https://nl.mouser.com/new/dfrobot/dfrobot-gravity-ozone-sensor

[34] Henan Hanwei Electronics Co.Ltd, "MQ131 Semiconductor Sensor for Ozone," MQ131 datasheet.

[35] AOSONG(Gangzhou) Electronics Co.Ltd., "Digital temperature and humidity sensor," AM2315 Product Manual.

[36] S. H. Ki, K. Masur, K. Y. Baik, and E. H. Choi, "Effects of humidity on room disinfection by dielectric barrier discharge plasma," *Journal of Physics D: Applied Physics*, vol. 52, no. 42, p. 425204, 2019.

[37] F. Avino, A. Howling, M. Von Allmen, A. Waskow, L. Ibba, J. Han, and I. Furno, "Surface dbd degradation in humid air, and a hybrid surface-volume dbd for robust plasma operation at high humidity," *Journal of Physics D: Applied Physics*, vol. 56, no. 34, p. 345201, 2023.

[38] J. D. McClurkin, D. E. Maier, and K. E. Ileleji, "Half-life time of ozone as a function of air movement and conditions in a sealed container," *Journal of Stored Products Research*, vol. 55, pp. 41–47, 2013. [Online]. Available: https://www.sciencedirect.com/science/article/pii/S0022474X13000659